OPEN

Correspondence and
requests for materials
should be addressed to
Z.M.Z. (zzm@ustc.
edu.cn) or Z.P.W.
(zpwang@ustc.edu.cn)

Thickness Dispersion of Surface Plasmon of Ag Nano-thin Films: Determination by Ellipsometry Iterated with Transmittance Method

Junbo Gong[1], Rucheng Dai[2], Zhongping Wang[2] & Zengming Zhang[2]

[1]Department of Physics, University of Science and Technology of China, Hefei, Anhui 230026, China, [2]The Centre of Physical Experiments, University of Science and Technology of China, Hefei, Anhui 230026, China.

Effective optical constants of Ag thin films are precisely determined with effective thickness simultaneously by using an ellipsometry iterated with transmittance method. Unlike the bulk optical constants in Palik's database the effective optical constants of ultrathin Ag films are found to strongly depend on the thickness. According to the optical data two branches of thickness dispersion of surface plasmon energy are derived and agreed with theoretical predication. The thickness dispersion of bulk plasmon is also observed. The influence of substrate on surface plasmon is verified for the first time by using ellipsometry. The thickness dependent effective energy loss function is thus obtained based on this optical method for Ag ultrathin films. This method is also applicable to other ultrathin films and can be used to establish an effective optical database for ultrathin films.

S urface plasmon, as a collective electron oscillation behavior in surface mode, has been extensively studied since the prediction by Ritchie[1]. The most common plasmonic material, silver, due to its wide optical and electrical application, has received amount of attention while there is still something obscure especially for ultrathin silver films[2–5]. For example, thickness dependence of surface plasmon of ultrathin films which was predicted in 1957 lacks straightforward optical experimental evidence ever since. The optical and dielectric properties of ultrathin silver films have significant difference from bulk material. One way to analyze surface plasmon is through energy loss function which can be deduced directly from optical constants, refractive index n and extinction coefficient k[6,7]. Generally, optical constants can be obtained either by optical methods[8] or by transmission/reflection electron energy loss spectroscopy (TEELS/REELS) techniques[8,9]. However, Palik's optical database in common use actually is not applicable to ultrathin films in thickness under several tens nanometers considering that it has been proved by many researchers that the optical constants of a film are dependent on thickness when the film is very thin[10,11]. This limitation has caused difficulty to surface analysis area as theorists working on surface electron spectroscopy have found that the simulation results with Palik's optical data can describe bulk material while have an obvious deviation with experimental results of thin films[12]. In fact, either optical or REELS measurements were almost all performed on single crystal Ag surface or bulk Ag[9]. However, actual applications based on surface plasmon generally use thin Ag films made of nanoparticles[13]. Study on ultrathin Ag film is significant for exploring the properties of thin film plasmon[14,15].

To achieve this purpose, firstly, the optical constants of ultrathin films need to be determined precisely. Even for better optical coating performance, it is necessary to study the thickness dependence of optical constants to extend the optical database from bulk to 2-dimension film; this requires the simultaneous determination of optical constants with film thickness. However, the extraction of optical data for ultrathin films from REELS spectra has not yet been performed because of the analysis difficulty and the need of clean thin film surface prepared *in situ*[2]. Therefore, the optical method should be more practically useful. Ellipsometry, as the most effective optical method to obtain optical constants, also faces a challenge when applied to ultrathin absorbing films. The traditional ellipsometry usually measures the change of amplitude and phase, i.e. $\tan\Psi(\lambda)$ and $\Delta(\lambda)$ respectively, of the polarized light of wavelength λ after reflection from the sample surface. The relationship between the ellipsometry parameters is $R_p/R_s = \tan\Psi \cdot \exp(i\Delta)$, where R_p and R_s are the complex reflection coefficients of polarized p- and s-waves, respectively, which are related with film thickness and optical constants
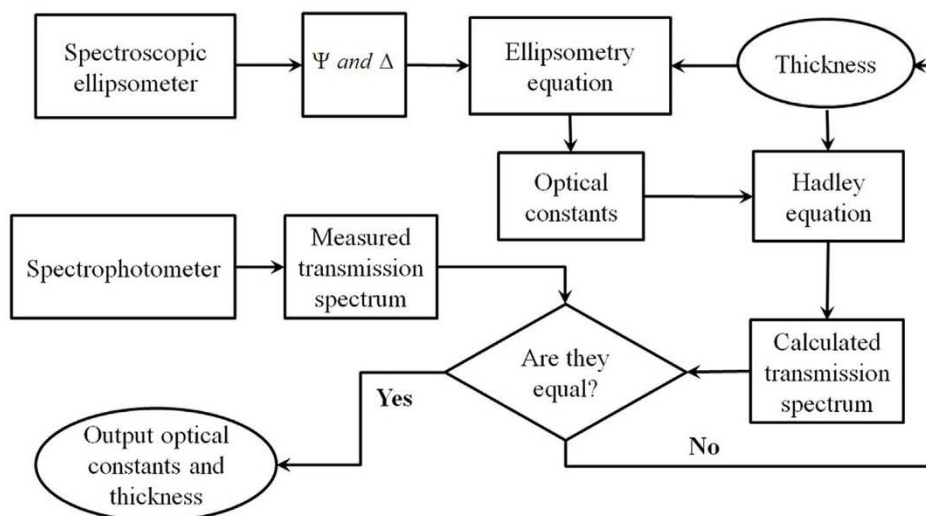
Figure 1 | **Schematic of ellipsometry iterated with transmittance method.**

by Fresnel equation. Solution of this complex equation (in total number of 2N where N is the number of wavelength spectrum channels) requires one of the quantities, i.e. film thickness d and optical constants ($n(\lambda)$ and $k(\lambda)$), is known. When film thickness and optical constants, in total number of $2N + 1$, are all unknown as in the present case, it is impossible to precisely determine them simultaneously due to lack of sufficient constraint equations. In fact, the non-uniqueness of solutions is the main problem with traditional ellipsometry. Therefore, a dispersion relationship for the dependence of optical constants on wavelength is usually assumed. However, there is no any suitable dispersion model for ultrathin metal films.

Results

In this paper, an ellipsometry iterated with transmittance method is proposed and has been used to determine effective optical constants of nano-thin films. The basic consideration is to supply additional N constrained equations with the help of the measured transmittance spectrum $T(\lambda)$. The flow chart of this method is shown in Fig. 1. First, with an initial thickness value assumed and the measured ellipsometric parameters, Ψ and Δ, the initial optical constants are obtained based on the ellipsometry equation. Then a transmittance spectrum is computed by using this initial thickness and the optical constants based on Hadley equation (Supplementary information). The calculated transmittance spectrum $T_{cal}(\lambda)$ is then compared with the measured spectrum $T_{exp}(\lambda)$. Here we use mean square error (MSE) to quantify the difference,

$$\mathrm{MSE} = \sqrt{\frac{1}{N}\sum_{i=1}^{N}\left[T_{exp}(\lambda_i) - T_{cal}(\lambda_i)\right]^2}. \quad (1)$$

The thickness value is then altered to minimize MSE. The iteration procedure is performed until a minimum MSE value is achieved, indicating that the final derived thickness value and optical constants altogether satisfy the ellipsometry equation and Hadley equation. Fig. 2(a) shows the measured transmittance spectra for ultrathin Ag film on quartz glass substrate samples at different effective film thicknesses whose values are obtained by above procedure. As an example shown by Fig. 2(b), the calculated spectrum is best matched with the experimental spectrum for the effective thickness value of 9.6 nm corresponding to minimum MSE. The self-consistent optical constants and film thickness can thus be precisely and simultaneously determined. Unlike the traditional ellipsometry dispersion

model is not necessary here. The resultant optical constants are unique.

However, it is necessary to point out that this method is based on the assumption of a uniform film on a substrate. The dielectric response of nanostructured materials to an external perturbation depends on significantly the sample morphology as boundary conditions of Maxwell's equation. For an ultrathin metal film in the form of metal islands on a substrate, the dielectric property is in fact that of the mixture of the islands and the embedding dielectric (the air here) and is hence connected with the surface roughness. To simplify the problem a concept of effective optical constants has been introduced within the limits of a homogeneous layer model[16]. Theoretical investigations have also treated heterogeneous media as homogeneous with some effective optical properties[17,18]. Here, we define an effective thickness and effective optical constants which can satisfy ellipsometry equation and Hadley equation simultaneously for ultrathin metal film in form of islands. In addition, considering that the size of optical beam in millimeters is much larger than that of islands, the film can be regarded as homogeneous on a macro-scale and thus the film properties can be described by the effective optical constants of the homogeneous layer. The same values of effective optical constants and of effective thickness measured at different positions of the sample also confirm that this assumption is suitable.

Fig. 3 shows the obtained refractive index $n(\lambda)$ and extinction coefficient $k(\lambda)$ in the wavelength range from ultraviolet to near infrared for silver ultrathin films at different thicknesses. The film with the thickness below 8 nm displays a non-metallic behavior considering that the value of refractive index is larger than that of extinction coefficient in wavelength range from 600 nm to 1000 nm (inset of Fig. 3). With increasing thickness the film changes to metallic behavior; the refractive index in range of 600-1000 nm gets larger at first from 4.7 nm thick and goes down from 6 nm thick and finally tends to be stable. Meanwhile the extinction coefficient monotonously increases with thickness while the increment gradually gets smaller. When the thickness is larger than 12 nm, both n and k tend to be stable and become closer to those of bulk Ag.

Discussion

In REELS analysis the bulk energy loss function (BELF), $\mathrm{Im}\{-1/\varepsilon\} = \varepsilon_2/(\varepsilon_1^2 + \varepsilon_2^2)$, and the surface energy loss function (SELF), $\mathrm{Im}\{-1/[1+\varepsilon]\} = \varepsilon_2/[(1+\varepsilon_1)^2 + \varepsilon_2^2]$, characterize the probability of electrons to undergo bulk excitation in volume and surface excitation in surface region, respectively[19], where ε_1 and ε_2 are the real and imaginary parts of dielectric constant ε. Figs. 4(a) and
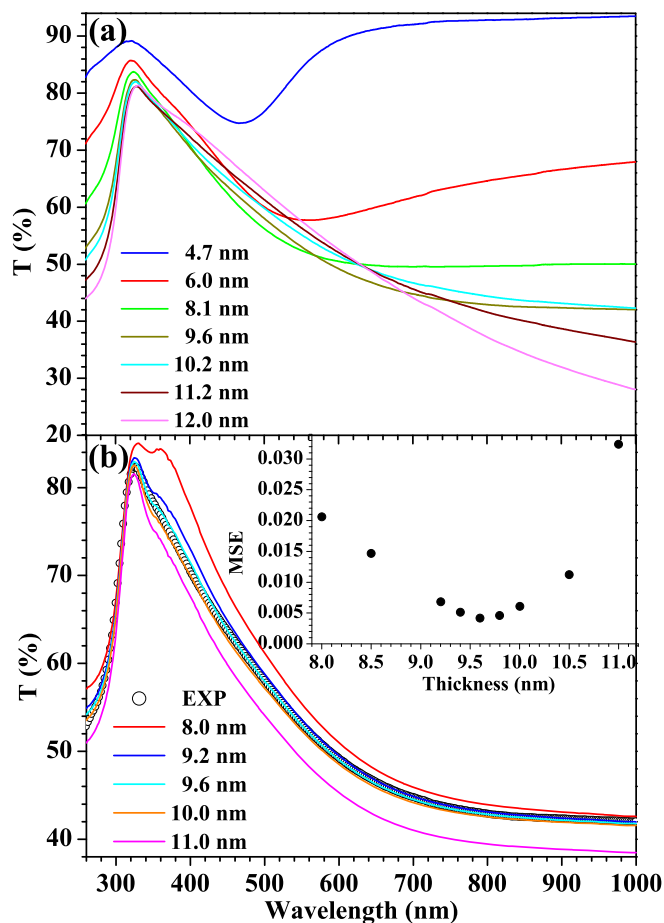
Figure 2 | (a) Measured transmittance spectra for ultrathin Ag film on quartz glass substrate samples at different effective film thickness; (b) Fitted transmittance spectra of 9.6 nm thick film assuming different thickness values (inset shows the corresponding MSE values of fitting results).

Figure 3 | **Dependence of the refractive index *n* (a) and extinction coefficient *k* (b) on the wavelength for silver films at different thicknesses.** Inset in Fig. (b) shows the optical constants *n* and *k* of films with 4.7 nm and 6.0 nm effective thickness.

4(b) display the plots of effective BELF and effective SELF, derived from the present effective optical constants, of Ag films as a function of the photon energy in ultraviolet region, which respectively show the bulk plasmon excitation peak and surface plasmon peak. The peak positions of the BELF and SELF for a thick film, which can be seen as bulk Ag for ellipsometry, are 327 nm (3.79 eV) and 338 nm (3.67 eV), respectively. For comparison, the corresponding bulk and surface plasmon energies of bulk material derived from Palik's database are, respectively, 3.81 and 3.68 eV[8].

The thickness dependence of peak positions of BELF and SELF is shown in Fig. 5. It is obvious that both of them shift to a higher energy side with increasing thickness. While the thickness dispersion of surface plasmon can be well explained by the theory, the thickness dependence of bulk plasmon energy reflects the fact that the optical constants of thin films contain information of electronic structure of films, which is different from that of bulk sample. The bulk plasmon frequency can be expressed in terms of the free electron density (ρ), the electron charge (e) and effective mass (m^*): $\omega_p = \sqrt{4\pi\rho e^2/m^*}$. Similar to the observation for indium thin film case[20], by increasing the film thickness the free electron density increases to reach the value of bulk silver, which agrees with the observed metallic behavior with thickness as deduced from the optical constants shown in Fig. 3.

It can be seen from SELF in Fig. 4(b) that there is an obvious shoulder at lower energy side beside the main surface plasmon peak. The position of the shoulder is determined by subtracting the sym-
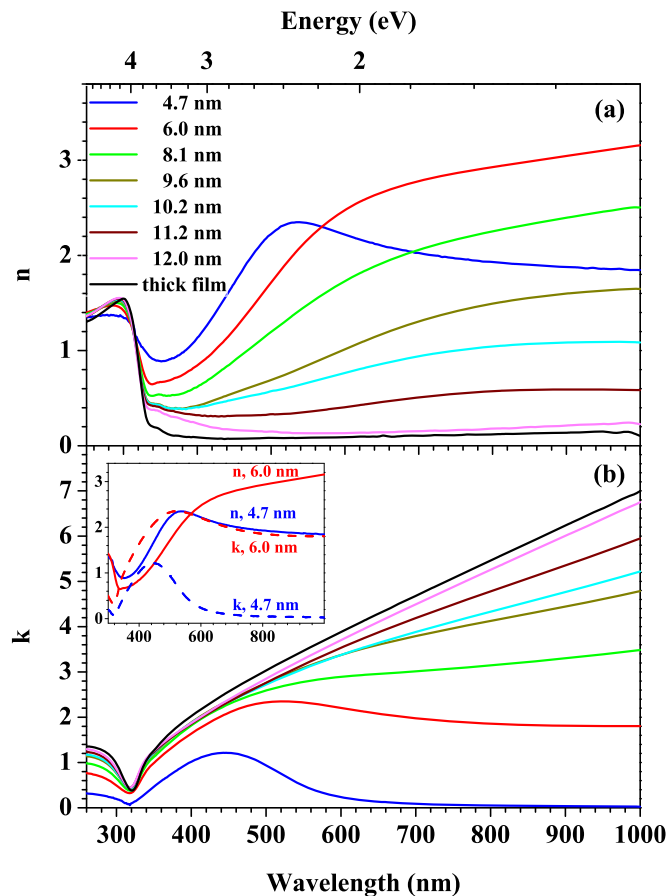
metric main peak as shown in the inset of Fig. 4(b). The main peak corresponds to surface plasmon at metal-to-air interface while the shoulder peak to the metal-to-substrate interface. The observation of shoulder peak provides a strong evidence for the existence of symmetric mode contributing from quartz glass substrate in ultrathin Ag films while the asymmetric mode is too weak to observe. Previous studies shows that the plasmon waves at the top and bottom surfaces of a film generate two different normal modes of higher and lower frequencies[21]. In the case of a free-electron metal film surrounded by a dielectric ε_a, the theoretical surface plasmon dispersion gives[1],

$$\omega_s^{\pm} = \omega_p \sqrt{\frac{1 \pm \exp(-qd)}{1 + \varepsilon_a}} \qquad (2)$$

where *d* is the thickness of a film and *q* the wave vector. For small *qd*, only the ω_s^- branch can exist[22]. In the present case, the metal film is surrounded by air ($\varepsilon_a = 1$) and quartz glass ($\varepsilon_a = 2.3$) by two sides; we assign the ω_{s1}^--branch for metal-to-air interface and ω_{s2}^--branch for metal-to-substrate interface. The thickness dispersion is fitted for two branches as, $\omega_{s1}^- = 0.97\omega_p\sqrt{1-e^{-0.52d}}$ and $\omega_{s2}^- = 0.94\omega_p\sqrt{1-e^{-0.30d}}$ where *d* is in nm, respectively. Quantitative difference of the observed surface plasmon energy with Eq. (2) is due mainly to non-free-electron-like behavior of silver film.

In fact, the film surface is not an ideally flat plane but made of particle islands as observed by atomic force microscopy (AFM) (Supplementary information, Figure S2). Therefore the above experimental result may also be qualitatively explained by another theoretical result[23]. AFM images indicate that the particle size relates with
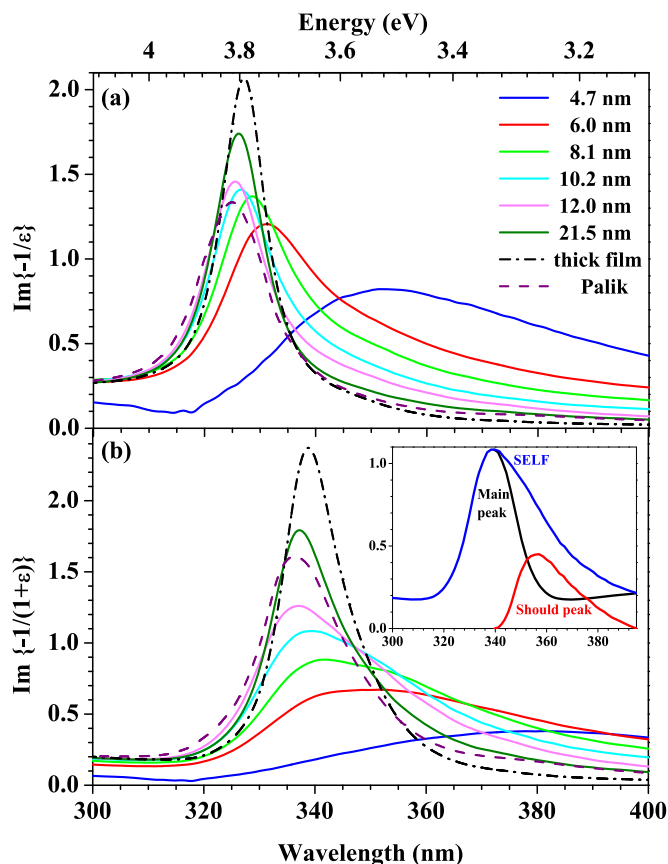
Figure 4 | The bulk energy loss function (a) and surface and energy loss function (b) in ultraviolet region for silver films at different thicknesses. Inset in Fig. (b) shows the determination of shoulder peak by subtracting the symmetric main peak.

Figure 5 | Thickness dependence of bulk plasmon and surface plasmon energies for silver films. (The red and blue fitted line represent the ω_{s1}^{-} - branch for metal-to-air interface and ω_{s2}^{-}-branch for metal-to-substrate interface, respectively. The red arrow marked the position of silver surface plasmon from Palik's database and the black one corresponding to volume plasmon.)

Methods

Ag of 99.99% purity was deposited on pre-cleaned quartz glass substrate to prepare the silver thin films by AC magnetron sputtering. The transmittance spectra from 260 nm to 1000 nm of the prepared Ag films were measured at normal incidence by a double-beam spectrophotometer (Shimazu Co., Inc. SolidSpec-3700). Ellipsometric spectra from 260 nm to 1000 nm were collected at incidence angles of 58° and 68° by a rotating-polarizer ellipsometer (J.A. Woollam Co., Inc. M-2000U). The ellipsometric spectra at two incident angles were used simultaneously in fitting ellipsometric parameters, Ψ and Δ.

the thickness, and the van der Drift model presents the proportional increasing behavior[24,25]. On the other hand, considering an isolated spherical particle (relative permittivity ε_r) surrounded by a dielectric medium of ε_a, the surface resonance condition is given by $\varepsilon_r = -\varepsilon_a(\ell+1)/\ell$, where ℓ is an integer[23]. For a free-electron-like metal, the surface plasmon frequency is $\omega_s = \omega_p / \sqrt{1+\varepsilon_a(\ell+1)/\ell}$. Here, the $\ell = 1$ is related to dipole mode oscillation, while $\ell = 2$ corresponds to the quadrupole oscillation, and so on. The resonance at lowest frequency corresponding to $\ell = 1$ dominates in very small particles. However, for larger nanoparticles where the dipole approximation is no longer valid, the resonance mode depends explicitly on the particle size[26]. The larger the particles become, the more important the higher order modes are because the electromagnetic field can no longer polarize the nanoparticles homogeneously as the particle size approach to the wavelength of the exciting radiation. As a conclusion, with increasing particle size the resonance frequency at higher order modes increases gradually; this results in the thickness dispersion of plasmon energy towards the value of bulk material for a thick film.

In conclusion, employing the ellipsometry iterated with transmittance method, the effective thickness and effective optical constants of thin Ag films deposited on quartz glass have been simultaneously obtained. The derived effective surface energy loss function and bulk energy loss function of Ag nano-thin films with different thicknesses have shown an obvious difference with that of Palik's data for single crystal silver. Thickness effect on the energy loss function has been discussed and the influence of substrate on surface plasmon energy predicted by Ritchie has also been observed. This optical measurement method based on ellipsometry is helpful to study effective energy loss function and plasmon properties of ultrathin films.
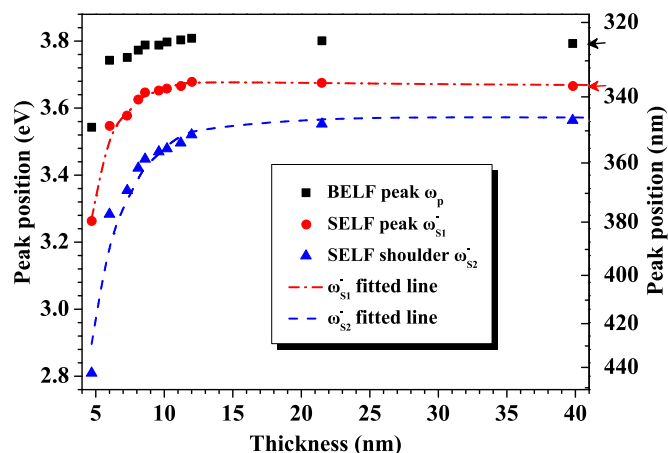
1. Ritchie, R. H. Plasma losses by fast electrons in thin films. *Phys. Rev.* **106**, 874–881 (1957).
2. Yu, Y. *et al.* Thickness dependence of surface plasmon damping and dispersion in ultrathin Ag films. *Phys. Rev. B* **72**, 205405 (2005).
3. Wang, H. N. & Zou, S. L. Extremely low scattering cross section of a perforated silver film. *Appl. Phys. Lett.* **94**, 073119 (2009).
4. Yoon, J. W., Koh, G. M., Song, S. H. & Magnusson, R. Measurement and modeling of a complete optical absorption and scattering by coherent surface plasmon-polariton excitation using a silver thin-film grating. *Phys. Rev. Lett.* **109**, 257402 (2012).
5. Wu, S. *et al.* Enhanced rotation of the polarization of a light beam transmitted through a silver film with an array of perforated s-shaped holes. *Phys. Rev. Lett.* **110**, 207401 (2013).
6. Ding, Z. J., Li, H. M., Pu, Q. R., Zhang, Z. M. & Shimizu, R. Reflection electron energy loss spectrum of surface plasmon excitation of Ag: A Monte Carlo study. *Phys. Rev. B* **66**, 085411 (2002).
7. Barnes, W. L., Dereux, A. & Ebbesen, T. W. Surface plasmon subwavelength optics. *Nature* **424**, 824–830 (2003).
8. Palik, E. D. *Handbook of optical constants of solids.* (Academic Press, New York, 1985).
9. Werner, W. S. M., Glantschnig, K. & Ambrosch-Draxl, C. Optical constants and inelastic electron-scattering data for 17 elemental metals. *J. Phys. Chem. Ref. Data* **38**, 1013–1092 (2009).
10. Heavens, O. S. Optical properties of thin films. *Rep. Prog. Phys.* **23**, 2 (1960).
11. Lehmuskero, A., Kuittinen, M. & Vahimaa, P. Refractive index and extinction coefficient dependence of thin Al and Ir films on deposition technique and thickness. *Opt. Express* **15**, 10744–10752 (2007).
12. Lambin, Ph., Senet, P. & Lucas, A. A. Validity of the dielectric approximation in describing electron-energy-loss spectra of surface and interface phonons in thin films of ionic crystals. *Phys. Rev. B.* **44**, 6416 (1991).
13. Nicoletti, *et al.* Three-dimensional imaging of localized surface plasmon resonances of metal nanoparticles. *Nature* **502**, 80–84 (2013).
14. Halas, N. J., Lal, S., Chang, W. S., Link, S. & Nordlander, P. Plasmons in strongly coupled metallic nanostructures. *Chem. Rev.* **111**, 3913–3961 (2011).
15. Ghosh, S. K. & Pal, T. Interparticle coupling effect on the surface plasmon resonance of gold nanoparticles: From theory to applications. *Chem. Rev.* **107**, 4797–4862 (2007).
16. Stenzel, O., Wilbrandt, S. & Kaiser, N. *Effective optical constants of evaporated silver and copper island ultrathin films. Optical Interference Coatings, OSA Technical Digest.* (2013) Available at: http://dx.doi.org/10.1364/OIC.2013.WA.10. (Accessed: 8th November 2014).

17. Garahan, A., Pilon, L. & Saxena, I. Effective optical properties of absorbing nanoporous and nanocomposite thin-films. *J. Appl. Phys.* **101**, 014320 (2007).
18. Hutchinson, N., Navid, A., Coquil, A. & Pilon, L. Effective optical properties of highly ordered mesoporous thin films. *Thin Solid Films* **518**, 2141–2146 (2010).
19. Tougaard, S. Accuracy of the non-destructive surface nanostructure quantification technique based on analysis of the XPS or AES peak shape. *Surf. Interface Anal.* **26**, 249–269 (1998).
20. El-Oker, M. M., Sultan, F. A., Yousef, S. A. & El-Sahhar, S. A. Surface plasmon modes and energy loss function of indium thin films on mica substrates. *Phys. Stat. Sol. A* **83**, 263–267 (1984).
21. Stern, E. A. & Ferrell, R. A. Surface plasma oscillations of a degenerate electron gas. *Phys. Rev.* **120**, 130 (1960).
22. Summerside, P. & Mahanty, J. Retarded dispersion interaction between metals. *Phys. Rev. B* **19**, 2944 (1979).
23. Raether, H. *Surface plasmons on smooth and rough surfaces and on gratings.* (Springer Berlin, Heidelberg, 1988).
24. Thijssen, J. M. Simulations of polycrystalline growth in 2 + 1 dimensions. *Phys. Rev. B* **51**, 1985 (1995).
25. Zhang, X., Song, X. H. & Zhang, D. L. Thickness dependence of grain size and surface roughness for dc magnetron sputtered Au films. *Chin. Phys. B* **19**, 086802 (2010).
26. Fujimoto, F. & Komaki, K. I. Plasma oscillations excited by a fast electron in metallic particle. *J. Phys. Soc. Jpn.* **25**, 1679–1687 (1968).

Author contributions

J.B.G. and Z.M.Z. conceived and designed the experiments. J.B.G. prepared the figures and wrote the manuscript with the assistance from all authors. R.C.D. and Z.P.W. participated in supervising the work. All authors reviewed the manuscript.

Additional information

Supplementary information accompanies this paper at http://www.nature.com/scientificreports

Competing financial interests: The authors declare no competing financial interests.

How to cite this article: Gong, J.B., Dai, R.C., Wang, Z.P. & Zhang, Z.M. Thickness Dispersion of Surface Plasmon of Ag Nano-thin Films: Determination by Ellipsometry Iterated with Transmittance Method. *Sci. Rep.* **5**, 9279; DOI:10.1038/srep09279 (2015).